PLOS Pathogens

RESEARCH ARTICLE

Comparative virulence analysis of seven diverse strains of *Orientia tsutsugamushi* reveals a multifaceted and complex interplay of virulence factors responsible for disease

Panjaporn Chaichana[1], Naphat Satapoomin[2], Chitrasak Kullapanich[2], Suthida Chuenklin[3], Aisha Mohammad[4], Manutsanun Inthawong[5], Erin E. Ball[5], Thomas P. Burke[6], Piyanate Sunyakumthorn[5], Jeanne Salje[1,2,7,8]*

1 Cambridge Institute for Medical Research, University of Cambridge, Cambridge, United Kingdom, **2** Mahidol-Oxford Tropical Medicine Research Unit, Faculty of Tropical Medicine, Mahidol University, Bangkok, Thailand, **3** Nuffield Departmnt of Medicine, University of Oxford, Oxford, United Kingdom, **4** Public Health Research Institute, Rutgers the State University of New Jersey, Newark, New Jersey, United States of America, **5** Department of Veterinary Medicine, Walter Reed Army Institute of Research-Armed Forces (WRAIR-AFRIMS), Bangkok, Thailand, **6** Department of Microbiology and Molecular Genetics, University of California, Irvine, School of Medicine, Irvine, California, United States of America, **7** Department of Biochemistry, University of Cambridge, Cambridge, United Kingdom, **8** Department of Pathology, University of Cambridge, Cambridge, United Kingdom

* jss53@cam.ac.uk

Check for updates

OPEN ACCESS

Citation: Chaichana P, Satapoomin N, Kullapanich C, Chuenklin S, Mohammad A, Inthawong M, et al. (2025) Comparative virulence analysis of seven diverse strains of *Orientia tsutsugamushi* reveals a multifaceted and complex interplay of virulence factors responsible for disease. PLoS Pathog 21(6): e1012833. https://doi.org/10.1371/journal.ppat.1012833

Editor: Jason A Carlyon, Virginia Commonwealth University School of Medicine, UNITED STATES OF AMERICA

Received: December 16, 2024

Accepted: May 27, 2025

Published: June 30, 2025

Copyright: © This is an open access article, free of all copyright, and may be freely reproduced, distributed, transmitted, modified, built upon, or otherwise used by anyone for any lawful purpose. The work is made available under the Creative Commons CC0 public domain dedication.

Data availability statement: The authors confirm that all data underlying the findings are

Abstract

Orientia tsutsugamushi is an obligate intracellular bacterium found in *Leptotrombidium* mites that causes the human disease scrub typhus. A distinguishing feature of *O. tsutsugamushi* is its extensive strain diversity, yet differences in virulence between strains are not well defined nor well understood. We sought to determine the bacterial drivers of pathogenicity by comparing seven strains using murine infections combined with epidemiological human data to rank each strain in terms of relative virulence. Murine cytokine expression data revealed that the two most virulent strains, Ikeda and Kato, induced higher levels of IL-6, IL-10, IFN-γ and MCP-1 than other strains, consistent with increased levels of these cytokines in patients with severe scrub typhus. We sought to identify the mechanistic basis of the observed differential virulence between strains by comparing their genomes, *in vitro* growth properties and cytokine/chemokine induction in host cells. We found that there was no single gene or gene group that correlated with virulence, and no clear pattern of *in vitro* growth rate that predicted disease. However, microscopy-based analysis of the intracellular infection cycle revealed that the only fully avirulent strain in our study, TA686, differed from all the virulent strains in its subcellular localisation and expression of its surface protein ScaC. This leads us to a model whereby drivers of pathogenicity in *Orientia tsutsugamushi* are distributed throughout the genome, likely in the large and varying arsenal of effector proteins encoded by different strains, and that these interact in

fully available without restriction. All relevant data are within the paper and its Supporting information files.

Funding: This work was supported by a Wellcome Trust Senior Research Fellowship (224277/Z/21/Z to JS and PC), an NIH R21 award (R21AI144385 to JS and PC) and an NIH R56 award (R56AI148645 to JS and PC). The funders had no role in study design, data collection and analysis, decision to publish, or preparation of the manuscript.

Competing interests: The authors have declared that no competing interests exist.

complex ways to induce differing immune responses and thus differing disease outcomes in mammalian hosts.

Author summary

Scrub typhus is a vector-borne human disease caused by the bacterium *Orientia tsutsugmushi* and spread by mites. There are numerous different strains of this bacterium with some causing severe disease in humans, and others that have not been found in human patients at all. The factors driving these differences are not yet understood, and gaining insight into them could aid in vaccine development and help predict the severity of disease caused by new isolates. To better determine the mechanistic basis of pathogenicity in scrub typhus, we carried out experiments in which we compared seven diverse strains for virulence in animals. We measured their ability to cause disease in mice, so that we could reliably classify them as virulent or avirulent in this model. We then analysed various genomic and biological aspects to identify disease markers in both mice and humans. The data suggest that there is no single factor that predicts whether a strain will be pathogenic or not, but that disease in scrub typhus is a complex process resulting from the activity of multiple bacterial genes working together to drive different immune responses in the host, resulting in either clearance of the bacteria from the host, or escalating disease. Future work exploring the relationship of bacterial effector proteins will help to disentangle this complex relationship in mechanistic detail.

Introduction

Scrub typhus is a severe vector-borne human disease caused by the obligate intracellular bacterium *Orientia tsutsugamushi* (Ot, Order Rickettsiales, Family Rickettsiaceae) [1–3]. Clinical manifestations include headache, fever, and rash, and if not treated promptly and with effective antibiotics this can escalate to multiple organ failure and death. Scrub typhus is a leading cause of severe febrile illness in many parts of Asia, particularly in rural regions, while related species causing scrub typhus-like disease have recently been described in other parts of the world, namely *Candidatus* Orientia chiloensis in Chile [4–6] and *Candidatus* Orientia chuto in the Middle East [7]. The primary arthropod reservoir and vector of Ot is the *Leptotrombidium* mite, where it is found in the salivary glands and ovaries and can be transovarially transmitted.

A key outstanding question in the field is: what bacterial factors drive disease outcomes in scrub typhus? The determinants of virulence for a particular Ot strain are likely to be encoded within the bacterial genome. Ot has an unusual genome of 2.1-2.8 Mbp, in which around 50% of the genome is comprised of multiple copies of an amplified and highly degraded mobile genetic element, the integrative

and conjugative element named the rickettsial amplified genetic element (RAGE) [8–10]. All strains used in the current study have complete genome sequences available and a detailed analysis of these genomes found that the sequences in between the RAGEs, called inter-RAGEs (IRs) are highly conserved between Ot strains, although the ordering of the groups of IR genes along the genome varies substantially [11]. All genomes encoded 76–93 RAGEs, although these are mostly heavily degraded with some as short as three genes in length. Whilst the classes of genes encoded in RAGEs are consistent between genomes, there is substantial variation in the numbers of different genes. In particular, Ot encodes large numbers of Ankyrin repeat containing proteins (Anks) and tetratricopeptide repeat containing proteins (TPRs), both of which are predicted effector proteins, with enormous diversity in their number and primary amino acid sequence [11]. Whilst the biological function of certain Anks has been determined [12–17], and the subcellular localisation of all the different Anks in strain Ikeda have been shown [12], no function has been determined for the majority. In summary, Ot genomes are complex and some secreted effector proteins have been described [12–17], however, the genetic determinants of pathogenicity in the genomes of Ot strains remains largely unknown.

Ot enters host cells using a combination of clathrin-mediated endocytosis and micropinocytosis [18,19], whereupon it escapes the endolysosomal pathways and is located directly in the host cytoplasm. It traffics to the perinuclear region using dynein-dependent motility along microtubules [20], driven by an interaction between the bacterial surface autotransporter protein ScaC and the dynein adaptor proteins BicD1/BicD2 [21]. Ot undergoes bacterial replication in the perinuclear region over a period of 3–7 days. It then exits infected cells by relocating to the host cell surface and budding off, encased in host plasma membrane [22]. This mode of exit is unusual amongst intracellular bacteria, and it is associated with a developmental transition to a distinct extracellular form of Ot [18]. Whilst aspects of this intracellular infection cycle were discovered in different strains, reflecting the main strain used by different laboratories, a comparison of the similarities and differences in the infection cycle between different strains of different virulence has not been reported.

This study investigates the mechanistic basis of pathogenicity caused by Ot. We carried out a side-by-side comparison of the relative virulence of seven diverse Ot strains in a murine model of disease and combined this with analyses of the *in vitro* growth properties of the same strains in multiple cell types. We also measured cytokines elicited by each strain *in vitro,* performed genome comparisons of virulence genes, and characterized the intracellular lifecycles of these strains by fluorescence microscopy. Together, these studies suggest that virulence is not encoded by a single gene, or group of genes, but is distributed across the genome of Ot and that disease severity results from a complex interplay between Ot factors and the host immune response to this infection.

Results

A combination of murine and human infection data leads us to classify seven Ot strains into a hierarchy of relative virulence based on specific criteria

It is unknown why some Ot strains are more virulent than others. To address this, it was important to first determine whether the strains differ in virulence and therefore we conducted large scale murine infection experiments using 7–8 different Ot strains. Previous comparative studies using murine infection models have examined only two or three strains, making it difficult to rank a larger number by virulence [23–26].

We performed two experiments, one with a high infection dose of 10^7 per mouse and a shorter duration of 8 days, and a second with a lower infection dose of 1.25 x 10^6 per mouse and a longer duration of 12 days (Fig 1A–1E). Both experiments used 6–9 week old C57BL/6NJ (low dose) or C57BL/6NJcl (high dose) mice and intravenous inoculation. The strains used in our study were Karp, Kato, Gilliam, UT76, Ikeda, TA686 and TA763 [10]. We additionally used UT176 in some experiments to enable comparisons to our previous work that used this strain [23]. Both TA686 and TA763 were originally isolated from animals [27], whilst all the other isolates originate from human patients. Karp, Kato and Gilliam are the three main serotypes found in Southeast Asia [27,28], UT76 and UT176 were isolated from patients in Northern Thailand [29] and Ikeda is a strain prevalent in Japan [30].

Ikeda and Kato caused significant weight loss and lethality in the high dose experiment (Fig 1A and 1B). In the low dose experiment, only Kato caused lethality (S1 Fig) but Kato, Ikeda and UT76 all caused a small but significant weight loss during the course of infection (Fig 1C). By comparison, lethality and significant weight loss was not observed in any other strain in either experiment (Fig 1A, 1B and 1C). The bacterial levels in the blood at the time of termination were correlated with weight loss and lethality in the high-dose experiment, with UT76, Ikeda, and Kato exhibiting the highest levels of bacteremia. (Fig 1D). In the low-dose experiment, although UT76, Ikeda, and Kato all exhibited the highest levels of bacteremia, UT76 levels were significantly higher than those of the other two strains, indicating that the animals were less able to clear this particular strain (Fig 1E).

We sought to compare these data with previous studies to better categorise the seven strains. Murine studies have shown that Karp, Kato, and UT76 are virulent, while Gilliam's virulence varies with the mouse strain, classifying it as intermediate [23,24,26]. A study using silvered leaf monkeys compared the relative virulence of Karp, Kato, Gilliam, TA678 and TA686 [31]. It was shown that Karp, Kato and Gilliam caused illness in these animals, with some lethality observed in both Karp and Gilliam. By contrast, TA678 induced only limited clinical manifestations, and TA686 no clinical signs at all as measured by fever, lymphadenopathy, eschar formation or leucocytosis. Comparing disease outcomes in human patients infected with different strains is challenging due to factors like underlying health, initial bacterial load, and treatments received. However in a study in Hainan Island, Southern China, higher bacterial loads were observed in patients infected with Karp compared to Gilliam, while patients infected with TA763 had extremely low levels [32]. Similarly a study in South Korea showed more severe clinical features in patients infected with a South Korean isolate Boryong compared with Karp [33]. We carried out an analysis of the phylogeny of available *tsa56* gene sequences in the NCBI database to establish the distribution of strains reported from humans (Fig 1F and S2 Table). This gene is typically used to classify Ot strains, and most of the sequences deposited in this database are derived from human clinical studies. Therefore, this analysis gives some indication of the abundance of different strains causing disease in humans. Whilst the distribution of strains is biased by the geographical location of research activity, it is notable that the numbers of strains with >90% identity to Gilliam was close to that of Ikeda, UT76 and Karp. Out of 4,710 sequences analyse there were none identified with ≥98% identity to TA686, suggesting this strain is not found in humans (Fig 1F).

Based on these data, we classify Kato, Ikeda, UT76, UT176 and Karp as virulent because they produced bacteraemia and weight loss in the mouse model and are found in human patients. Of these, we classify Kato as the most virulent strain, followed by Ikeda and then UT76, based on lethality in the mouse model. Since Gilliam and TA763 did not cause weight loss or lethality, but are found in human patients, we classify these as strains with intermediate virulence, as has been described before for Gilliam. Finally, the fact that TA686 had no significant weight loss or mortality, combined with its demonstrated lack of virulence in a non-human primate study and its absence from databases of human patient isolates (Fig 1F), suggests that this strain is avirulent. There is a relationship, albeit not absolute, between this virulence classification and the phylogenetic relationships (S1 Table and [10]). The two most virulent strains, Kato and Ikeda, are closely related, whilst the other virulent strains UT76, Karp and UT176 also group together phylogenetically. Gilliam, TA686 and TA763 are more distantly related to those strains and to each other.

Different Ot strains exhibit different tissue tropism

The tissue tropisms of the different Ot strains remained unclear. We compared the tissue tropism of eight Ot strains by carrying out qPCR analysis of the brain, heart, kidney, lung, liver and spleen of all the animals in the high dose experiment (Fig 1G) Broadly speaking, the bacterial load in tissues correlated with virulence, whereby bacterial levels were generally lower in the avirulent and intermediate virulent strains compared with the virulent strains. Among internal organs the brain showed the lowest bacterial loads with mean values of 87 – $9.5x10^4$ Ot copies per mg, and lung and spleen the highest with mean values of 94 - $7x10^6$ and 880 – $1.9x10^7$ Ot copies per mg respectively (Fig 1G). There were some notable strain-specific outliers. In UT176 the level in the heart was as high as in the lung and spleen, whilst Kato was comparatively abundant in the brain.

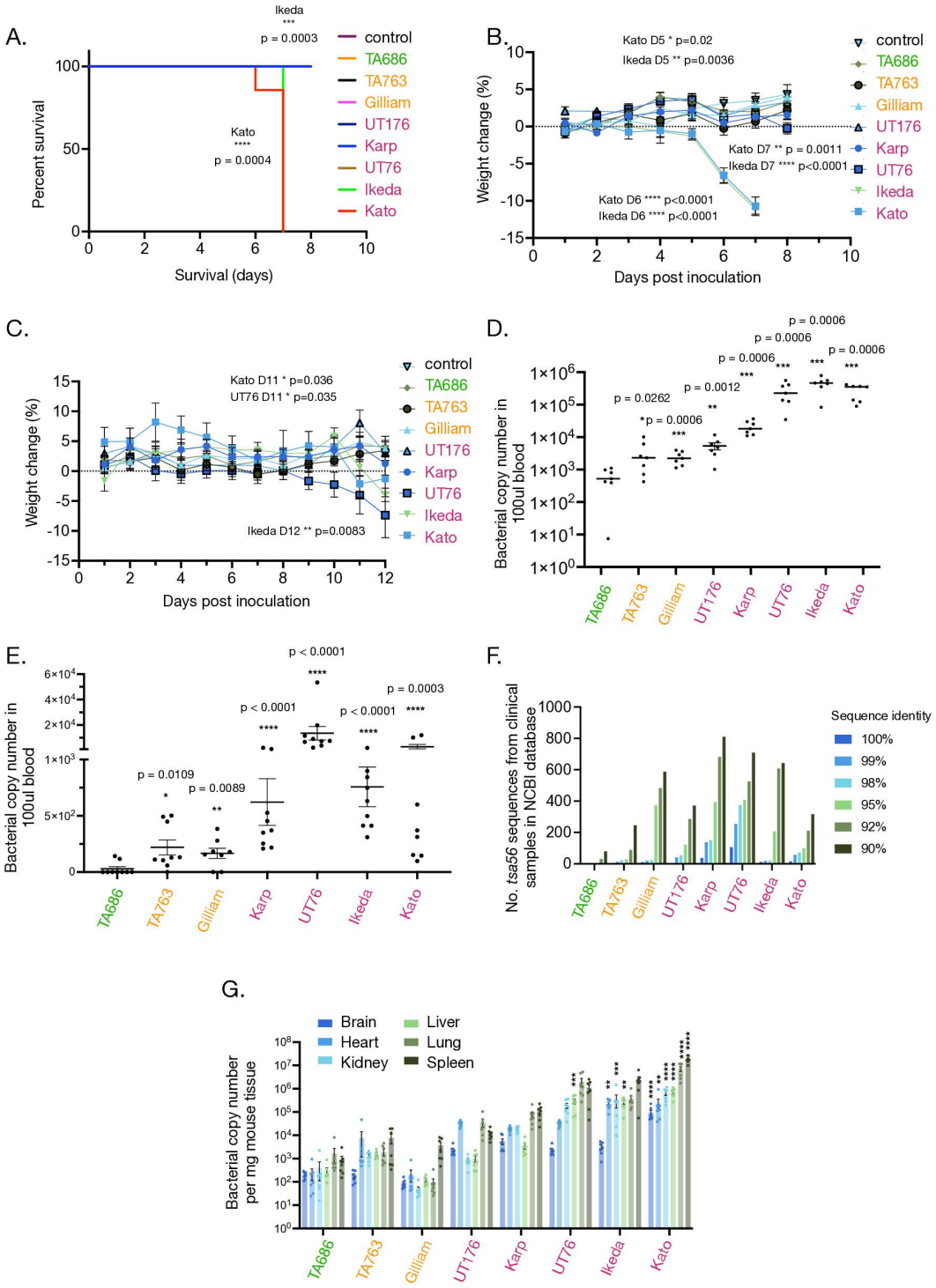


Fig 1. Ot strains can be classified into avirulent, intermediate virulent, and virulent groups. A-B. Results from high dose experiment in which C57BL/6NJcl were infected with 1x10^7 bacteria per animal and monitored for 8 days. A. Kaplan-Meier survival curves of mice infected with different bacterial strains showing that only strains Kato and Ikeda cause lethal infection in this animal model. Statistical significance was determined using log-rank Mantel-Cox analysis. B. Graph showing percentage weight change over time, whereby only strains Kato and Ikeda cause significant weight change during the course of infection. Percentage changes in body weight of Ot inoculated groups were compared to mock control by two-way ANOVA followed by Dunnet's multiple comparisons. Graph shows mean and SEM. C. Results from low dose experiment in which C57BL/6NJ were infected with 1.25x10^6

bacteria per animal and monitored for 12 days. Graph showing percentage weight change over time, whereby strains UT76, Kato and Ikeda cause small but significant weight change during the course of infection. Percentage changes in body weight of Ot inoculated groups were compared to mock control by two-way ANOVA followed by Dunnet's multiple comparisons. Graph shows mean and SEM. D-E. Bacteremia in high dose (D) and low dose (E) experiment. Graph shows bacterial load in mouse blood at point of termination as measured by qPCR using primers against the conserved single copy bacterial gene *tsa47.* Mean and SEM are shown. Statistical significance was determined using Mann Whitney test in which each strain was compared with TA686. The lowest measured value in these experiments was 7.4 bacteria per 100 μl blood. F. Numbers of DNA sequences of the Ot-specific gene *tsa56* available on the NCBI database on 1 July 2024 with 90%, 92%, 95%, 98% and 100% sequence identity to the *tsa56* sequence from different Ot strains used in our study. Sequences in the NCBI database are almost entirely derived from clinical samples, so this analysis reflects the global levels of strains related to the strains in our study present in reported clinical studies. G. Bacterial load in different mouse tissues at the point of termination as measured by qPCR using primers against the conserved single copy bacterial gene *tsa47.* Mean and SEM are shown. Statistical significance was determined using ordinary one-way ANOVA followed by Dunnett's multiple comparisons tests to TA686. * $p \leq 0.05$, ** $p \leq 0.01$, *** $p \leq 0.005$, **** $p \leq 0.0001$.

https://doi.org/10.1371/journal.ppat.1012833.g001

Ot strains elicited distinct immune responses in a murine infection model

The main driver of pathogenesis in human scrub typhus disease is an overactivation of the inflammatory response leading to disseminated intravascular coagulation and tissue damage [34,35]. We previously compared two strains, Karp and UT176 (distinct from UT76 used in the current study) and found that Karp caused greater disease severity in a mouse model of infection, and induced more proinflammatory cytokines including IL33 in a dual RNAseq analysis of Ot-infected HUVEC cells [23]. A different study compared the virulence of Karp and Gilliam and two murine strains, C57BL/6 and outbred CD1 and found that both caused disease in CD1 but only Karp caused disease in C57BL/6 [26]. In the C57BL/6 mouse strain, Karp caused a stronger immune activation, including infiltration of CD4+ and CD8 + T cells and increased serum cytokine/chemokine levels compared with Gilliam.

We sought to explore how the multiple different Ot strains caused inflammation *in vivo*. We used Luminex profiling of serum taken at 6 days post infection in the high dose cohort to analyse the relative levels of 9 cytokines and chemokines: IL-1α, IL-1ß, IL-6, IL-10, IL-12(p70), IL-17, CCL2/MCP-1, GM-CSF and IFN-γ (Fig 2). MCP-1, IL-6 and IFN-γ exhibited a pattern that strongly correlated with virulence, whereby the avirulent and intermediate virulence strains TA686, TA763 and Gilliam induced low levels, while the virulent strains UT76 and Karp induced high levels, and high virulence strains Kato and Ikeda induced very high levels of cytokine. IL-10 showed the same pattern although no cytokine was detected in TA763. The virulent strain UT176 showed no induction of IL-17, IL12(p70), IL-10, IL-6, IL-1ß, IL-1a and IFN-γ suggesting a generally reduced inflammatory response relative to other strains. GM-CSF was upregulated relative to the control to a similar extent in all strains, as was IL-1a with the exception of UT176 that did not induce any detectable cytokine. IL-17, IL-12(p70) and IL-1ß were differentially upregulated in different strains without any patterns that correlate with virulence. Together, these data show that different strains lead to different signatures of inflammatory responses *in vivo*, but that relative induction of MCP-1, IL-6, IL-10 and IFN-γ correlates with degree of virulence in a murine infection model. Previous analysis of severe scrub typhus in human patients have shown that these same cytokines and chemokines are associated with severe disease in humans [36–40].

Comparative genomics reveals complexity of potential virulence genes in Ot

We sought to identify genetic determinants of pathogenicity in the genomes of Ot strains. First, we compared the RAGE regions of the Ot genome, that are composed of a highly proliferated integrative and conjugative element and make up around 50% of the Ot genome. We were not able to identify any patterns in the number or completeness of RAGEs that correlate with virulence (Fig 3). We then examined the distribution of predicted effector proteins of the Ankyrin repeat (Ank) protein families, that are abundant within Ot RAGEs. We examined a published analysis of the 54–75 Ank genes present across Ot strains [11] and could not identify any patterns of distribution that correlated with virulence. However, there is extensive diversity in the arsenal of Anks encoded by Ot genomes, resulting in differential abilities to interact with host cells.

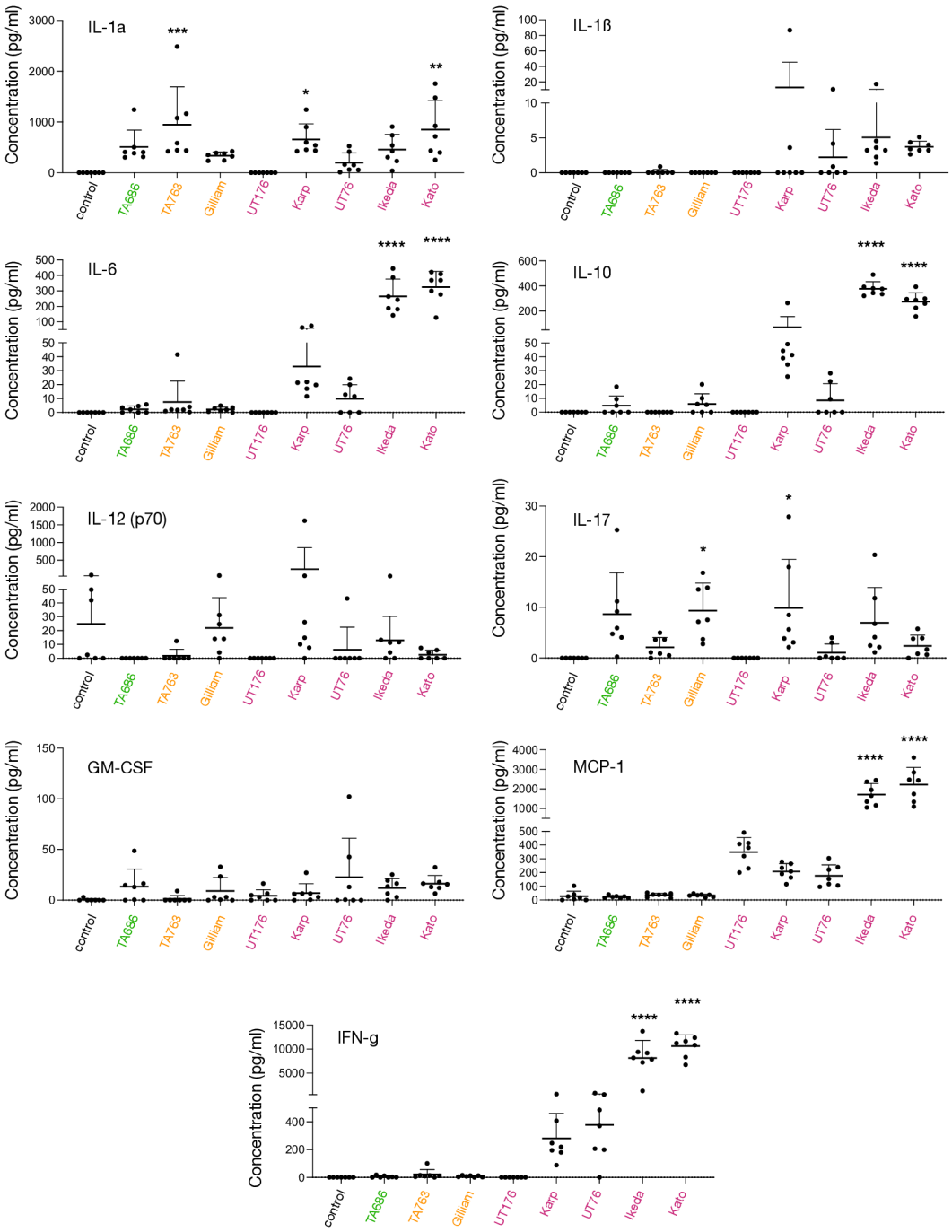


Fig 2. Cytokine profiling reveals a positive association of IL-6, IL-10, IFN-γ and MCP-1 with virulence in a murine infection model. Graphs show the relative levels of nine chemokines and cytokines in mouse blood collected from the tail vein at six days post infection in the high dose experiment described in Fig 1, as measured by Luminex analysis. Statistical significance was determined using one way ANOVA test followed by Tukey's multiple comparisons test in which all groups were compared with mock infected control. * $p < 0.05$, *** $p < 0.005$, **** $p < 0.0001$.

https://doi.org/10.1371/journal.ppat.1012833.g002

We then compared the non-RAGE regions of the different Ot strains to identify genes uniquely present or absent in pathogenic strains. The non-RAGE genes are encoded in small groups called inter-RAGE blocks (IRs) that are non-syntenous between strains due to the presence of very high numbers of RAGEs. We observed that the avirulent strain

	TA686	TA763	Gilliam	UT176	Karp	UT76	Ikeda	Kato
Genome size (Kbp)	2,254	2,279	2,465	1,932	2,470	2,078	2,009	2,319
Total ORFs	2,582	2,388	2,745	2,123	2,614	2,283	2,222	2,443
Number of RAGEs	93	nd	91	72	77	71	76	81
Number of complete RAGE	0	0	3	0	0	0	0	1
Number of IR regions	103	nd	95	96	84	86	91	92

gene name	region		accession number							
phrB	IR2	*deoxyribodipyrimidine photo-lyase*	*karp_00010*	-					-		
hypo	IR7		*karp_00271*	-		-				-	
xthA2	IR7	*exodeoxyribonuclease III*	*karp_00272*	-		-					
	IR10	*transcriptional regulator*	*karp_00333*			-					
hypo	IR14		*karp_00401*	-	-		-				
hypo	IR17		*karp_00457*		-	-			-		-
hypo	IR24		*karp_00651*		-	-				-	-
hypo	IR24		*karp_00652*		-	-			-	-	-
	IR26	*RNA binding protein*	*karp_00702*	-						-	
hypo	IR27		*karp_00710*				-				
hypo	IR31		*karp_00839*		-		-			-	-
	IR37	*propionyl-coA carboxylase b-domain*	*karp_00943*	-							
	IR37	*propionyl-coA carboxylase b-domain*	*karp_00944*	-						-	
	IR37	*propionyl-coA carboxylase b-domain*	*karp_00945*	-		-			-	-	-
	IR37	*Acetyl/propionyl coA*	*karp_00947*	-		-				-	
hypo	IR37		*karp_00948*				-		-	-	
accC	IR37	*biotin carboxylase*	*karp_00949*	-		-	-			-	-
hypo	IR38		*karp_01013*			-					
hypo	IR40		*karp_01079*			-					
hypo	IR45		*karp_01168*		-		-		-		
acnA	IR59	*aconitate hydratase A*	*karp_01472*	-	-						
acnA	IR59	*aconitate hydratase A*	*karp_01473*	-		-			-		
	IR62	*ATPase AAA*	*karp_01529*	-	-	-					
leuS	IR62	*leucine tRNA ligase*	*karp_01530*	-		-					
	IR70	*phosphoribosylaminoimidazolesuccinocarboxami*	*karp_02128*							-	-
hypo	IR74		*karp_02214*						-		
VirB2-3	IR76		*karp_02232*		-					-	
hypo	IR77		*karp_02262*	-	-	-	-		-		
hypo	IR78		*karp_02311*		-	-				-	-
hypo	IR81		*karp_02405*		-		-			-	-
hypo	IR81		*karp_02424*	-	-	-	-			-	
IR15 hypo	IR15		TA686_01374		-			-			
IR10 hypo	IR10		Ikeda_01549		-			-			
IR10 hypo	IR10		Ikeda_01525					-			
IR10 hypo	IR10		Ikeda_01522				-	-	-		-
IR59 hypo	IR59		Ikeda_00824					-			
IR55 hypo	IR55		Ikeda_00578	-	-	-	-	-	-		-
IR20 hypo	IR20		Ikeda_01972		-		-				
IR23 hypo	IR23		Ikeda_02041	-		-	-	-			
strB	IR85	streptomycin-6-phosphotransferase	Kato_01559		-	-	-	-	-		
	IR85	dienelactone hydrolase	Kato_01560		-	-	-	-	-		
	IR85	ester cyclase	Kato_01561		-	-	-	-	-		
	IR86	DNA gyrase inhibitor	Kato_01562	-	-	-	-	-	-		
	IR86	DNA gyrase inhibitor	Kato_01563	-	-	-	-	-	-		
IR86 hypo	IR86		Kato_01564		-	-		-	-		
IR86 hypo	IR86		Kato_01565	-	-	-		-	-		
IR86 hypo	IR86		Kato_01566	-	-	-		-	-		
IR86 hypo	IR86		Kato_01567	-	-	-		-	-		
fosA	IR86	Glutathione transferase FosA	Kato_01568	-	-	-		-	-	-	
ubiE	IR86	Ubiquinone/menaquinone biosynthesis C-	Kato_01569	-		-	-	-	-		
IR86 hypo	IR86		Kato_01570	-	-	-	-	-	-		
mutT	IR86	DNA mismatch repair protein MutT	Kato_01571	-	-	-	-	-	-		
	IR86	Aminoglycoside N(6')-acetyltransferase type 1	Kato_01572	-	-	-	-	-	-		
MarR	IR86	MarR family transcriptional regulator	Kato_01573	-	-	-	-	-	-		
fabG	IR86	3-ketoacyl-ACP reductase	Kato_01574	-	-	-	-	-	-		
	IR86	ABC transporter permease	Kato_01575	-	-	-	-	-	-		
AraC	IR86	AraC family transcriptional regulator	Kato_01576	-	-	-	-	-	-		
	IR86	N-acetyltransferase	Kato_01577	-	-	-	-	-	-		
IR86 hypo	IR86		Kato_01578		-						
	IR86	GNAT family N-acetyltransferase	Kato_01579	-	-	-		-	-		
IR86 hypo	IR86		Kato_01580	-	-	-		-	-		
IR86 hypo	IR86		Kato_01581	-	-	-	-	-	-		
	IR86	Kynurenine formamidase	Kato_01582	-	-	-	-	-	-	-	
IR86 hypo	IR86		Kato_01583	-	-	-	-	-	-		
IR40 hypo	IR40		Boryong_00903	-	-	-	-	-	-	-	-
aceF	IR64	dihydrolipoamide acetyltransferase	Boryong_01564	-	-	-	-	-	-	-	-
IR59 hypo	IR59		Boryong_01608	-	-	-	-	-	-	-	-
IR59 hypo	IR59		Boryong_01609		-	-		-	-		
IR77 hypo	IR77		Boryong_01720	-	-	-	-	-	-	-	-

Fig 3. Identification of genes whose presence/absence correlates with virulence. The presence or absence of any inter-RAGE genes not uniformly present across all eight genomes included in this analysis are shown. Green lines highlight genes uniquely absent in TA686 whilst magenta lines highlight those genes uniquely present in Ikeda and Kato. The inter-RAGE region in which the gene is located is shown in column 2. Additional information about each genome is given at the top of the table. ORF = open reading frame, RAGE = Rickettsial Amplified Genetic Element, IR = Inter-RAGE region.

https://doi.org/10.1371/journal.ppat.1012833.g003

TA686 contains the largest number of IRs, due to increased fragmentation of IRs compared to other genomes. However, the total number of virulent and avirulent genomes in our analysis is not sufficient to determine whether this is a virulence-related correlation. We analysed the identity of IR genes and identified 657 core genes present in all Ot genomes, and an additional 74 IR genes missing in one or more genomes. We analysed all 74 to seek patterns that correlate with virulence (Fig 3). We identified 2 genes uniquely absent in the avirulent strain TA686. These were propionyl-coA carboxylase b-domain gene and aconitate hydratase A. These genes are not known to be associated with pathogenicity in other organisms, although it is possible that their absence in TA686 is associated with a decreased survival *in vivo*. A lack of genetic tools makes it difficult to further test the relevance of these genes in virulence at the current time. We did not identify any genes that were present in all virulent strains compared with those of intermediate or no virulence. However, there were 19 genes uniquely found in Kato and Ikeda, the two most virulent strains. All but one are located in a single IR block, IR86, present only in these two strains. It is possible that the presence of this additional block of genes leads to increased bacterial growth and/or pathogenesis *in vivo.* However, it is important to note that Kato and Ikeda are more closely related to each other than to other strains in our study and therefore it is possible that this difference reflects genetic relatedness and has no impact on virulence. A larger number of genomes as well the availability of genetic tools will enable further studies on the relevance of these genes.

Ot strains grow at similar rates in macrophages and other cell types in vitro

In the case of the sister genus, *Rickettsia,* an inability to grow in macrophage cells is associated with a lack of pathogenicity [41,42], and we therefore hypothesized that *in vitro* growth rates of Ot strains would vary in different cell types in vitro. We measured the growth rate from 4-7 days in a mouse fibroblast cell line L929, a mouse macrophage cell line Raw264.7, mouse bone marrow derived macrophages (BMDMs), a dog macrophage cell line DH82, a human macrophage cell lines THP1, and human derived primary macrophages (Fig 4A). The growth rates were highly similar between strains, with no significant differences that correlated with virulence. These data suggest that differential virulence in Ot is not determined by intrinsic differential bacterial growth rates in certain cell types, unlike related pathogens.

Differential growth in interferon-activated macrophages does not explain differential virulence in Ot

IFN-γ is an anti-microbial cytokine that is upregulated in scrub typhus patients and was recently shown to be critical for controlling Ot *in vivo* [43], as well as *Rickettsia parkeri* in macrophages *in vitro* [44] and *in vivo* [45]. We therefore hypothesized that it may differentially restrict Ot strains *in vitro* based on their virulence *in vivo*. We measured intracellular bacterial abundance in the presence or absence of IFN-γ in four macrophage cell lines and primary cell types (Fig 4B). We found that stimulation with IFN-γ caused either no change or a slight decrease in bacterial growth in BMDMs and RAW264.7s. However, the observed differences did not correlate with measured differences in virulence *in vivo.* We therefore concluded that differential ability of Ot strains to replicate in IFN-γ stimulated macrophages is not the primary driver of differential virulence *in vivo.*

Cellular activation by IFN-γ leads to differences in the relative chemokine and cytokine induction by different strains of Ot, but these do not correlate with virulence

Our *in vivo* findings showed that the more virulent strains induced higher levels of IL-6, IL-10, IFN-γ and MCP-1 (Fig 2). This motivated us to determine whether we could determine any differences in chemokine and cytokine production *in vitro* that correlate with virulence. Therefore, we measured the production of cytokines and chemokines in mouse (Fig 5A) and human (Fig 5B) primary macrophages, both in the presence and absence of IFN-γ. We used RT-qPCR to determine the relative transcript levels of IL-6, TNF-alpha, IL-1ß, IL-33, CCL2/MCP-1, CCL4/MIP-1b, CCL5/RANTES, CXCL9 and CXCL10 in both uninfected cells and cells infected with seven different Ot strains, in the presence or absence of IFN-γ.

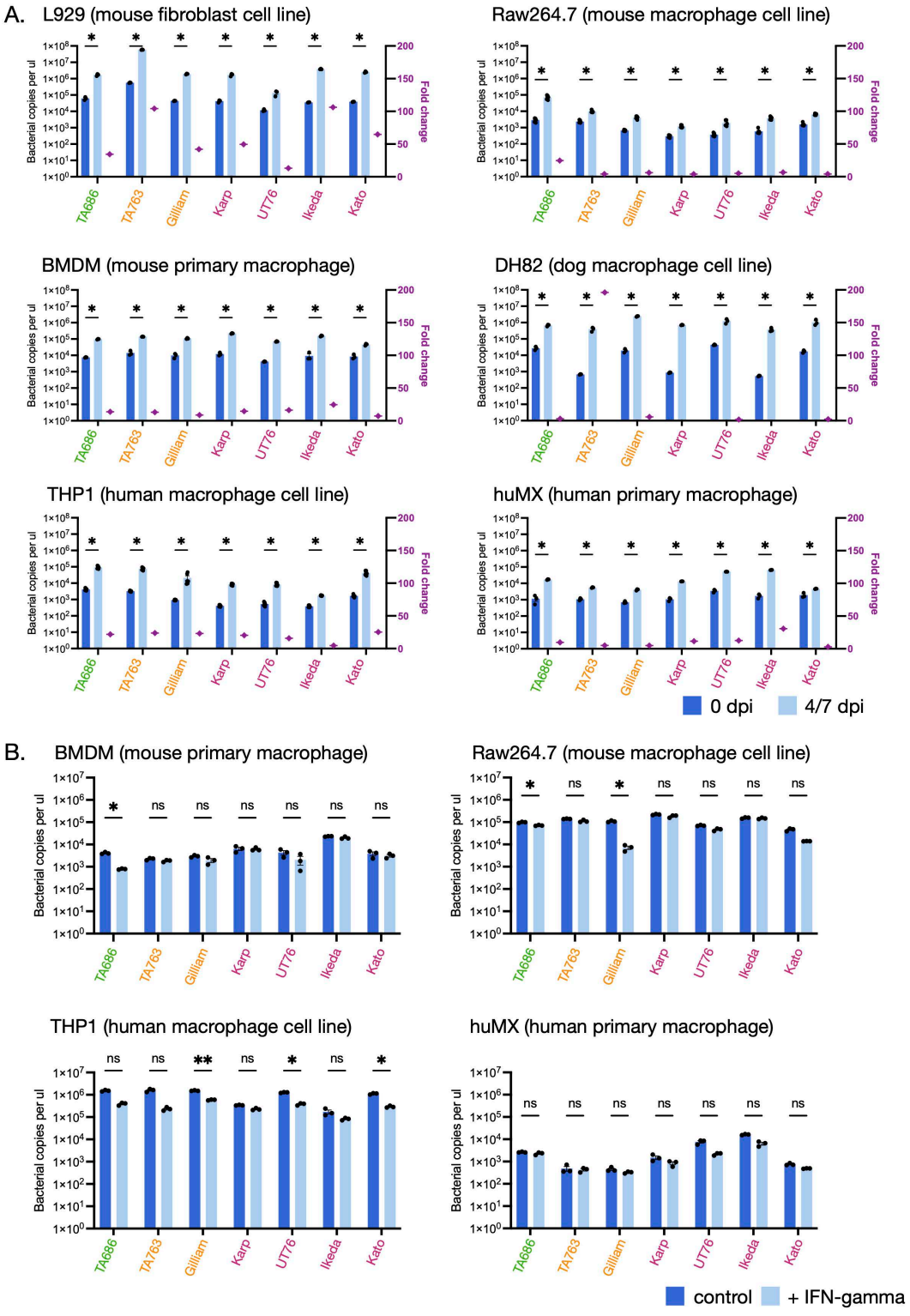


Fig 4. The *in vitro* growth rates of different Ot strains are similar to each other. A. Growth of seven strains in L929, Raw264.7, BMDM, DH82, THP1 and huMX cells. Bacteria were grown in different cell lines for 7 days (DH82) or 4 days (other cell lines). Bacterial levels were measured by qPCR using primers against the Ot-specific gene *tsa47*. Data are shown as mean ± SEM (n = 6); statistical significance of growth increase for each strain

was calculated using t -test where *, $p < 0.05$; **, $p < 0.01$, ***, $p < 0.005$. B. Growth of seven strains in BMDM, Raw264.7, THP1 and huMX cells in the presence and absence of IFN-γ.Bacteria were grown in different cell lines for 4 days. Bacterial levels were measured by qPCR using primers against the Ot-specific gene *tsa47* and the graph shows the bacterial level after 4 days growth in the presence or absence of 100U/ml of recombinant mouse or human IFN-γ. Data are shown as mean ± SEM (n = 3). The statistical significance of the difference between growth in the presence or absence of IFN-γ across strains within one cell line was determined using two-way ANOVA followed by Bonferroni's multiple comparisons, where *, $p < 0.05$; **, $p < 0.01$.

https://doi.org/10.1371/journal.ppat.1012833.g004

We found that infection with all strains of Ot upregulated the expression of IL-6, TNF-alpha, IL-1ß, and CXCL-10 (human macrophages only) both in the presence and absence of IFN-γ. We observed that for TNF-alpha, IL-33, CCL5/RANTES in mouse macrophages and IL-6, TNF-alpha, CCL2/MCP-1, CCL4/MIP-1b and CXCL9 in human macrophages, all Ot strains supressed the relative increase in expression upon IFN-γ expression. Exceptions from these trends included a high induction of mouse IL-6, IL-1B, IL-33 and human TNF-α and CCL5/RANTES by Ikeda, and high induction of mouse CCL2/MCP-1 by TA686. Taken together, the analysis revealed a heterogenous distribution of relative induction of cytokines and chemokines by different strains, differential effect of IFN-γ stimulation on different strains, and differential results in different cell lines and host species.

The avirulent strain TA686 differs from other strains in subcellular localisation and expression of surface autotransporter protein ScaC

It remained unclear if the intracellular infection cycles of Ot differed between strains. We compared the number and localization of Ot in cultured mouse fibroblast cells (L929) at four days post infection, at which point bacteria are undergoing active replication, and observed differences in subcellular localisation in TA686 compared with other strains (Fig 6A). While other bacteria were primarily located in a tight clump in the perinuclear region, or a mixture of tight perinuclear clump and diffuse cytoplasmic location, TA686 has a distribution that is primarily in the cytoplasm with 54% of infected cells exhibiting bacteria dispersed throughout the cytoplasm, compared with 4–21% of cells in other strains (Fig 6B). We repeated the comparison between Karp and TA686 in three other cell lines, human umbilical vein endothelial primary cells HUVEC, human retinal pigment epithelial cells Rpe1 and HeLa cells, and observed the same trend (S2 Fig).

We then hypothesized that the surface protein ScaC might be expressed differently across these strains and examined its expression patterns. We chose this protein as a marker for the intracellular infection cycle because previous research indicated it was found on only a small fraction of bacteria, primarily located outside host cells [18]. Thus, this differentially expressed protein could serve as a useful indicator for observing phenotypic differences between strains. We observed that there was very low ScaC expression on intracellular bacteria in six Ot strains grown in L929 cells, consistent with our extensive previous studies on this protein. By contrast, TA686 expressed high levels of ScaC in a large proportion of its bacterial cells at seven days post infection (Fig 6C and 6D). Together, these data show that the intracellular infection cycle of avirulent strain TA686 differs from all other Ot strains included in our study, though the relationship between these observations and virulence, as well as their generalizability to other avirulent strains, are unknown.

Discussion

The bacterium Ot, which causes the severe human disease scrub typhus, is notable for its wide diversity of strains. However, the drivers of human disease in this bacterium, and the reason why some strains are more virulent than others remains unknown. The major conclusion of this study is that each strain of Ot has a unique fingerprint of interactions with its host that results in different pathogenic outcomes in a manner that cannot currently be predicted from the bacterial genome sequence. A key unresolved question is whether analysing a larger number of Ot strains would reveal broad patterns, or if the diversity within Ot populations necessitates individual study for each new strain. We observed no obvious patterns in *in vitro* growth rate or inflammatory response that correlate with virulence, suggesting a complex interplay between multiple bacterial and host factors. However, we identified four chemokines and cytokines that correlate with

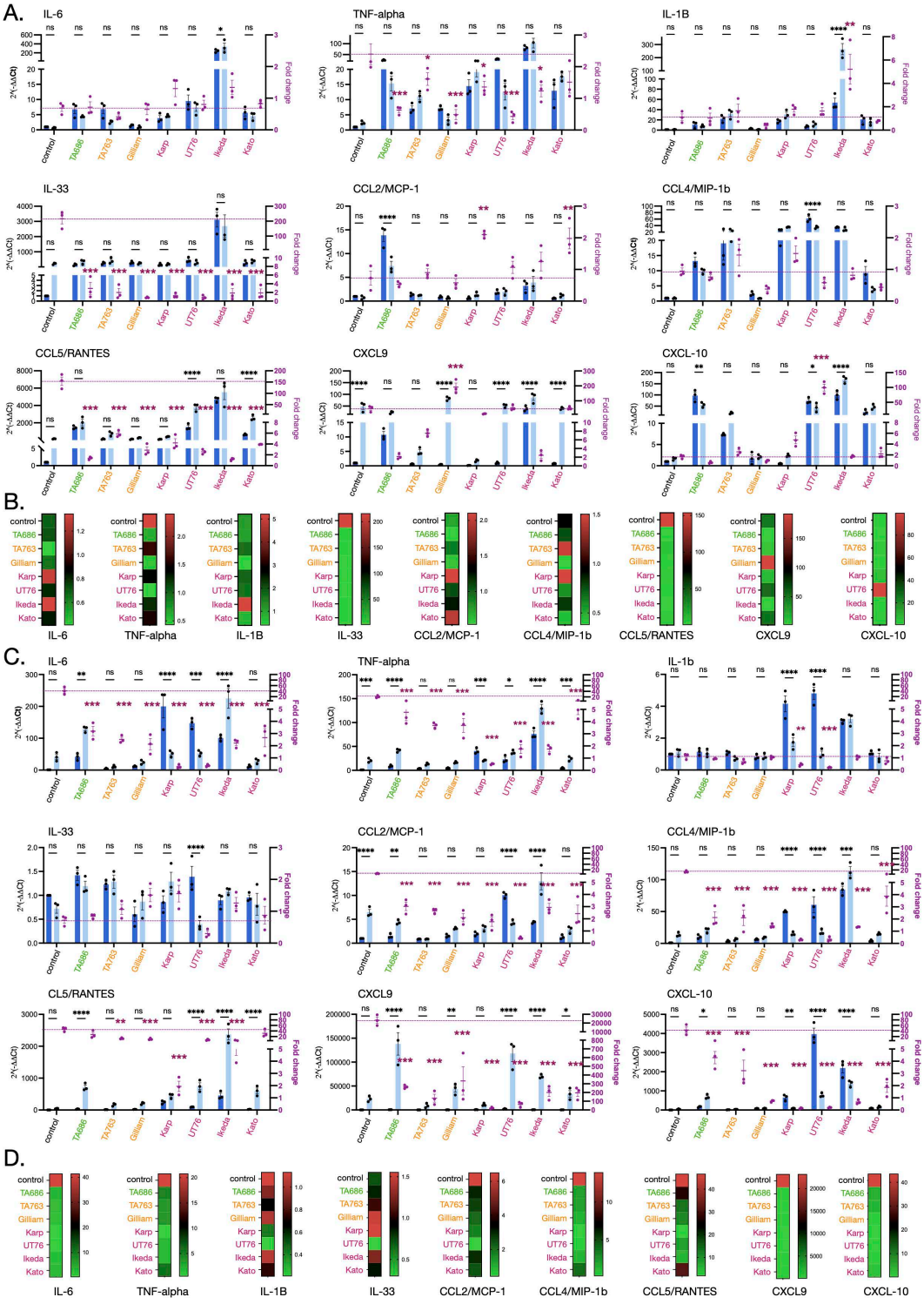


Fig 5. Different Ot strains induce different patterns of chemokine and cytokine induction in cultured macrophages. Graphs (A) and heatmaps (B) showing relative induction of nine chemokines and cytokines in response to infection with seven strains of Ot in murine bone marrow derived macrophages. Bacteria were infected in murine bone marrow derived macrophages for 4 days in the presence or absence of IFN-γ. The RNA was extracted and subjected to RT-qPCR using primers specific to different cytokines/chemokines. A. $2^{(-\Delta\Delta Ct)}$ (left Y-axis) and fold changes between the absence and presence of IFN-γ (right Y-axis). The statistical significance of the difference between cytokine/chemokines genes in the presence or absence of IFN-γ

across strains was determined using two-way ANOVA followed by Bonferroni's multiple comparisons, where *, $p < 0.05$; **, $p < 0.01$***, $p < 0.001$. Additional statistical tests comparing the significance of the fold change of cytokine gene expression in IFN-γ-treated infected cells compared with uninfected control was determined using two-way ANOVA followed by Tukey's multiple comparisons. Graphs (C) and heat maps (D) showing relative induction of nine chemokines and cytokines in response to infection with seven strains of Ot in human primary macrophages. Bacteria were infected in human primary macrophages for 4 days in the presence or absence of IFN-γ. The RNA was extracted and subjected to RT-qPCR using primers specific to different cytokines/chemokines. C. $2^{(-\Delta\Delta Ct)}$ (left Y-axis) and fold changes between the absence and presence of IFN-γ (right Y-axis). D. Heatmap. The statistical significance of the difference between cytokine/chemokines genes in the presence or absence of IFN-γ across strains was determined using two-way ANOVA followed by Bonferroni's multiple comparisons, where *, $p < 0.05$; **, $p < 0.01$, ***, $p < 0.001$. Additional statistical tests comparing the significance of the fold change of cytokine gene expression in IFN-γ-treated infected cells compared with uninfected control was determined using two-way ANOVA followed by Tukey's multiple comparisons.

https://doi.org/10.1371/journal.ppat.1012833.g005

virulence in a murine *in vivo* infection model: MCP-1, IL-6, IL-10 and IFN-γ. This finding is consistent with human disease studies [36–40] and confirms these molecules as markers of severity in scrub typhus.

The observation that different Ot strains vary substantially in their ability to cause disease in humans and mice likely reflects the fact that their primary reservoir is thought to be the *Leptotrombidium* mite, and not mammals. Mites feed on and infect rodents and other small mammals during the larval stage of its lifecycle [46–48]. Whilst Ot can be transmitted from mammals back to naïve mites, the efficiency is very low and rarely leads to the establishment of transovarial transmission in the previously uninfected mite [49]. Most of the lab strains of Ot were originally isolated from human patients or small animals and it is not known whether there is a separate large population of strains found in mites that are incapable of causing disease in humans. In the closely related genus *Rickettsia*, which includes various tick-borne human pathogens, recent metagenomic analyses of ticks have uncovered the presence of many previously unknown *Rickettsia* species which are not thought to cause disease in humans [50,51]. This suggests that most *Rickettsia* species have primarily evolved as endosymbionts of ticks, with only a small subset capable of causing human disease. It is unknown whether, by analogy, there are numerous yet undiscovered Ot strains that are only found in mites, but two lines of evidence point to this. First, target capture enrichment sequencing analysis showed diverse Ot strains in mites in Southeast Asia that are absent in human populations [52]. Second, an Ot-like species was recently reported from mites in North Carolina, USA, where no cases of scrub typus like illness have been described [53]. Thus, it is possible that large numbers of uncharacterized, nonpathogenic strains of Ot exist, reinforcing the notion that mammalian pathogenesis is a variable trait that is not integral to the biology of Ot.

It has previously been shown that the high levels of IFN-γ produced during Ot infection is essential for controlling disease, with a lack of IFN-γ in a murine model leading to lethal infection in an otherwise non-lethal model [43]. We examined the effect of IFN-γ stimulation of macrophages in our *in vitro* model and observed only a small decrease in bacterial growth rates that was independent of the virulence of the Ot strain indicating that the IFN-γ-mediated protection is not primarily due to increased bacterial killing by macrophages but rather the wider dysregulation in the immune response that was described in IFN-γ-deficient mice [43]. We showed that IFN-γ stimulation of mouse and human macrophages resulted in upregulation of numerous cytokines and chemokines, and that these effects were augmented or supressed differently by different strains. Therefore, the exact effect of the downstream immune response directed by IFN-γ *in vivo* will differ substantially between strains, driving different disease outcomes.

What are the strain-specific characteristics that drive the observed differences in immune response and thus virulence? We discuss three possible factors here. First, Ot encodes a large arsenal of predicted effector proteins in both the Ank and TPR family. Whilst a core subset of seven Anks are found in all eight Ot genomes analysed to date (Ank03, Ank08, Ank10, Ank11, Ank12, Ank20 and Ank24), there are an additional 122 Anks present in only a subset of strains [54]. Anks are Type 1 secreted effector proteins that localize to various compartments of the host cell and interact with different partners. For example, Ank01 and Ank06 of strain Ikeda modulate NF-kB relocation to the nucleus [15], whilst Ank13 of strain Ikeda is a nucleomodulin that modulates host gene transcription patterns [16]. The functions of most Ot Anks are unknown, but given

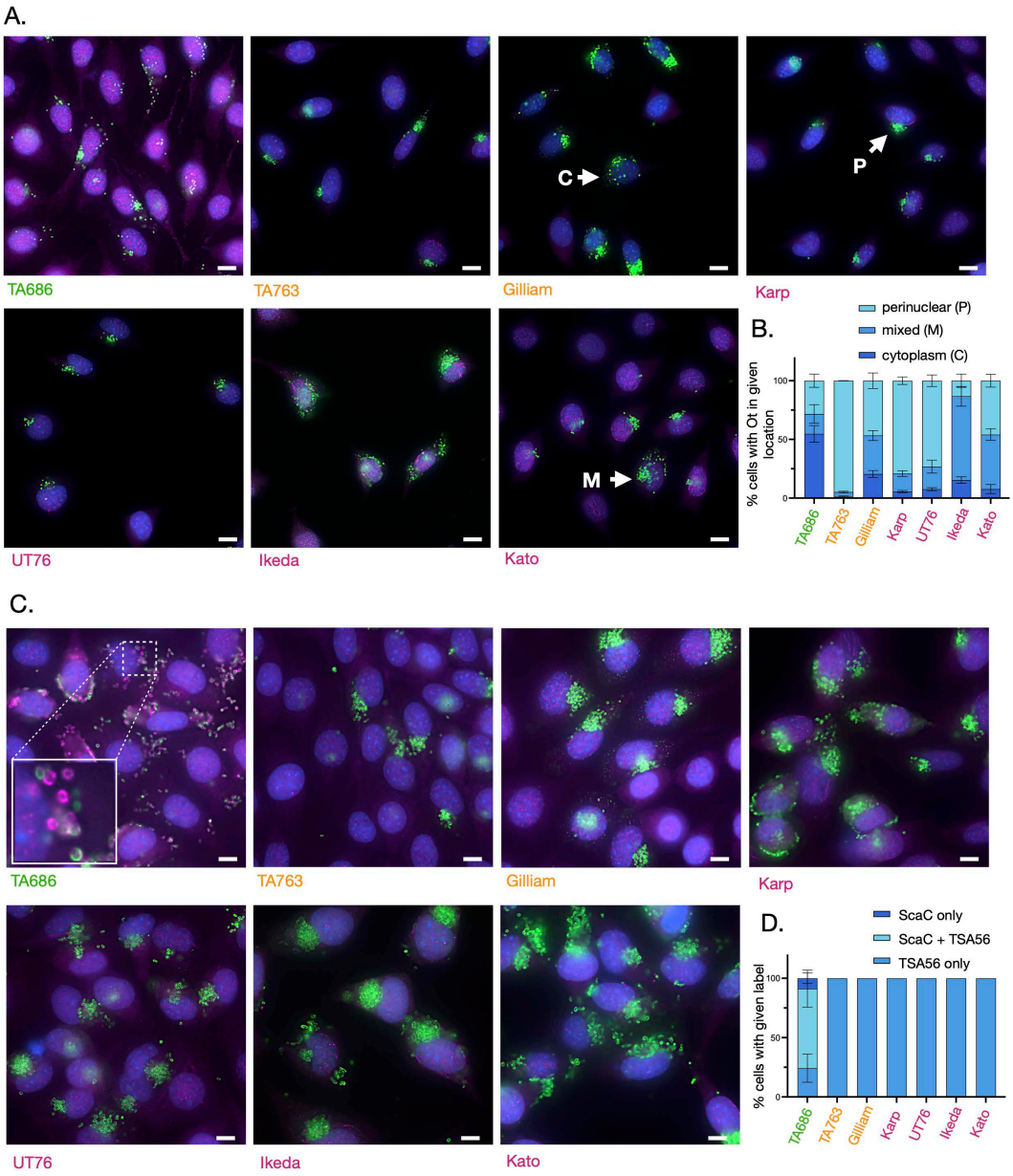


Fig 6. TA686 differs from other strains in its subcellular localisation and ScaC expression. Immunofluorescence microscopy images of seven strains of Ot infected with the same MOI and grown for 4 (A. and B.) or 7 (C. and D.) days in cultured L929 cells. Infected cells were fixed and labelled with an antibody against the abundant surface protein TSA56 (green) and the surface autotransporter protein ScaC (magenta). Host cell nuclei were labelled with Hoechst (blue). Scale bar = 10 μm. Representative images are shown in A. and C. whilst quantification is given in B. and D. Quantification was performed by manually scoring at least 50 infected cells from three independent replicates. In B. infected cells were scored as having bacteria in a perinuclear cluster, dispersed throughout the cytoplasm, or in both a perinuclear cluster and dispersed through the cytoplasm. In D. infected cells were scored as having bacteria inside them that were labelled with TSA56, ScaC, or both.

https://doi.org/10.1371/journal.ppat.1012833.g006

the diversity in Ank repertoire between strains it is likely that these account for significant strain specific differences in their ability to manipulate host cell biology. For example, Ank13 was shown to modulate the expression of multiple host genes including those involved in the inflammatory response. Out of the strains involved in our study Ank13 is only present in Ikeda, Kato and UT76 [11]. It is likely that there are other Ank proteins that also modulate different subsets of inflammatory genes and the exact combination of Anks with this activity present in a given strain will play a significant role in determining the host response to infection. The TPR proteins are less well understood than Anks, but the distribution of these effector proteins also differs significantly between strains. Together the scale and diversity of the Ank and TPR repertoire of Ot strains makes it highly likely that these play an important role in driving differential virulence. Second, despite a lack of obvious candidate virulence factors in the IR regions of the Ot genome, it is possible that strain specific differences in bacterial gene expression drive differences in host responses. Gene expression in bacteria is influenced by gene location within the genome, as differential supercoiling affects transcription and the gene's proximity to the origin of replication impacts its copy number during DNA replication.The highly unusual inter-strain rearrangement of the Ot genome may therefore result in differences in gene expression despite conservation of promoter sequences, and these may play a role in differential interactions with host cells and therefore virulence. Third, whilst all Ot strains studied to date encode a core genome of 657 conserved genes in their IR regions, it is possible that different alleles of these genes drive different outcomes during infection. For example, active site mutations or changes in protein-protein interaction sites might lead to altered activity of a biological pathway that cannot be predicted from a simplistic analysis of the presence or absence of a particular gene. Together, these three factors offer some plausible explanations for the observed strain specific differences in virulence.

Our comparative analysis led to the identification of one clear phenotype that correlates with virulence: the subcellular position and ScaC expression pattern of the avirulent strain TA686. The altered subcellular position may reflect a straightforward difference in bacterial mechanism, for example altered intracellular trafficking driven by a difference in activity of ScaC. However, it may also reflect a more substantial difference in the host cell, driven by the presence of different effector proteins, such as differential localization or activity of host derived systems involved in anchoring Ot to the perinuclear region. Whilst the relationship between bacterial subcellular position and virulence is unclear, this is the first reported bacterial phenotype that correlates with a lack of virulence and therefore a detailed analysis of its relationship will be the subject of future study. One important limitation of this finding is that we only included one avirulent strain in our study due to a strong bias towards human isolates in available strain collections, and therefore we cannot comment on the generalizability of this finding. The availability of a larger collection of avirulent strains, for example including those isolated from mites, would enable larger scale comparisons to be made.

Our understanding of Ot cell biology has come from concerted efforts from multiple labs across the world. Historically, different research groups have each worked on one or two Ot strains, often reflecting the geographic region where the research is based. One important conclusion from our study is that different Ot strains have different characteristics both at the level of *in vitro* cell biology and *in vivo* pathogenesis. Therefore, a greater emphasis on studying multiple strains would help the field to distinguish universal characteristics from strain specific features.

In summary, we have shown that different Ot strains exhibit differential virulence in a murine infection model and can be ranked into a hierarchy of virulence. We show that there is no single pattern of bacterial gene expression, *in vitro* growth rate, or inflammation that correlates with virulence, and we emphasize the importance of studying multiple different Ot strains. We show that the avirulent strain TA686 differs from other OT strains in its subcellular localization and ScaC expression, and hypothesize that this may be relevant in its differential virulence. We are hopeful that this study will help to drive forward the field of scrub typhus pathogenesis.

Materials and methods

Ethics statement

Experiment 1. This research was conducted in strict accordance with protocols approved by the Armed Forces Research Institute of Medical Sciences (AFRIMS) Animal Care and Use Committee, following Thai laws, the Animal Welfare Act, and all applicable U.S. Department of Agriculture, Office of Laboratory Animal Welfare, and U.S. Department of Defense guidelines. The approved protocol number was PN23–08. The animal research adhered to the Guide for the Care and Use of Laboratory Animals (8th Edition, NRC publication). AFRIMS is an AAALAC International-accredited facility located in Bangkok, Thailand.

Experiment 2. This research was conducted at the Rutgers Public Health Research Institute BSL3 vivarium facility, in strict accordance with protocols approved by the Institutional Animal Care and Use Committee (IACUC) at Rutgers University. The approved protocol number was PROTO202000012.

Cell culture and reagents

Bone marrow-derived macrophages (BMDMs) were isolated from 2-week-old male C57BL/6J mice and generously provided by Dr. Jelena Bezbradica Mirkovic. The murine monocytic cell line RAW264.7 was obtained from Dr. Samantha Bell. Mouse fibroblast cell line NCTC clone 929 (L-929) was purchased from ATCC (cat# CCL1).

BMDMs were cultured in DMEM-high glucose (Gibco, cat# 19650–62, Germany), supplemented with 10% fetal bovine serum (FBS; Gibco, cat# 16140071, USA), 1% Penicillin-Streptomycin-Glutamine (Gibco, cat# P4333, USA), 25 mM HEPES (Gibco, cat# 15630–056, USA), and 50 ng/ml Recombinant Mouse M-CSF (BioLegend, cat# 574806, USA). RAW264.7 and L929 cells were cultured in DMEM-high glucose, supplemented with 10% heat-inactivated FBS and 1% penicillin-streptomycin.

Human M1 macrophages (hMDM-GMCSF(-)) derived from a single donor were purchased from Promocell (cat# C-12914, Germany). These cells were cultured in M1-Macrophage Generation Medium XF (Promocell, cat# C-28055, Germany) according to the manufacturer's instructions. The human monocytic cell line THP-1, provided by Dr. Jason Yang, was cultured in RPMI-1640 medium (Sigma-Aldrich, cat# R0883, USA) supplemented with 10% heat-inactivated FBS and 1% Penicillin-Streptomycin-Glutamine (Gibco, cat# 10378–016, USA). All cells were maintained at 37°C in a 5% CO2 atmosphere.

Bacterial strains and propagation

Seven strains of *Orientia tsutsugamushi* were propagated in L929 cells following a previously described protocol [55]. Briefly, L929 cells were seeded in T75 flasks at a density of 3×10^6 cells per flask and incubated overnight before infection. A frozen bacterial stock was thawed and added directly to the flasks. On day 6 post-infection, the medium was removed, and the infected cells were washed once with Phosphate Buffered Saline (PBS; Gibco, cat# 10010023, Germany). The cells were then scraped from the flask, resuspended in PBS, and lysed using a bead mill homogenizer (Fisher Scientific, Finland) with glass beads at a power setting of 5 for 1 minute. Cell debris and glass beads were removed by centrifugation at 800 × g for 3 minutes. The supernatant containing bacteria was transferred to new tubes and subjected to high-speed centrifugation at 14,000 × g for 10 minutes to pellet the bacteria. The bacterial pellet was resuspended in Sucrose-Phosphate-Glutamate Buffer (SPG) and stored at -80°C until use.

Mouse experiments

Experiment 1. Female C57BL/6NJcl mice (lot numbers 9–18 and 9–22) were obtained from Nomura Siam International Co., Ltd. (Bangkok, Thailand) and used at 6–9 weeks of age. The mice were housed under specific pathogen-free (SPF) conditions in an animal biosafety level 2 (ABSL2) facility at AFRIMS. Mice were co-housed (4 mice per case, 2 cases per

group) in standard polycarbonate microisolator cages with filter tops and natural ventilation. Each cage was equipped with stainless steel feeding hoppers and water bottles, with temperature maintained at 21°C ± 1 and relative humidity between 30–70%.

Nine groups of mice (n = 7 per group) were intravenously injected via the tail vein (using insulin syringes, 30G, ½", BD Ultra-Fine II, Becton Dickinson) with 1×10^7 genomic DNA copies of different *Orientia tsutsugamushi* strains (TA686, TA763, Gilliam, UT176, Karp, UT76, Ikeda, and Kato), as well as a mock-infection control. To account for variations in bacterial viability, in vitro microscopy and qPCR experiments were conducted on all bacterial stocks used to confirm that the number of viable organisms was comparable between strains. Mice were weighed daily, and clinical signs of morbidity were monitored and scored over the 8-day experimental period. Mice displaying signs of severe morbidity or >15% weight loss from baseline were humanely euthanized. At the end of the study, blood and tissue samples (brain, heart, lungs, kidneys, spleen, and liver) were collected for bacterial quantification and histopathology. Mice were euthanized using CO_2 inhalation at a gas flow rate of 2 L/min at 15 psi CO_2, maintained for at least 5 minutes after cessation of breathing. Death was confirmed by physical examination (absence of a heartbeat), followed by an adjunctive physical method such as cervical dislocation or exsanguination.

Experiment 2. Female C57BL/6NJ mice were obtained from The Jackson Laboratory (ME, USA) and used at 6–9 weeks of age. The mice were housed under specific pathogen-free (SPF) conditions in an animal biosafety level 3 (ABSL3) facility.

Eight groups of mice (n = 9 per group) were intravenously injected via the saphenous vein with 1.25×10^6 genomic DNA copies of different *Orientia tsutsugamushi* strains (TA686, TA763, Gilliam, Karp, UT76, Ikeda, and Kato), as well as a mock-infection control. Mice were weighed daily, and clinical signs of morbidity were monitored and scored over the 12-day experimental period. Mice displaying signs of severe morbidity or >15% weight loss from baseline were humanely euthanized. At the end of the study, blood and tissue samples (brain, heart, lungs, kidneys, spleen, and liver) were collected for bacterial quantification and histopathology. Mice were euthanized via cervical dislocation and death was confirmed by prolonged observation and absence of heart beat.

Luminex analysis

Mouse immune responses were assessed using the MILLIPLEX multiplex assay (MCYTOMAG-70K, Merck Millipore) to measure nine analytes (GM-CSF, IFN-γ, IL-1α, IL-1β, IL-6, IL-10, IL-12(p70), IL-17, MCP-1), following the manufacturer's instructions. Cytokine quantification was performed on a MAGPIX (Luminex) analyzer, and data were collected using Belysa immunoassay software 1.2.2.

In vitro growth rate analysis

Cells were seeded overnight at 1 or 3×10^4 cells/well in 96- or 48-well plates, respectively. The following day, the medium was removed, and bacteria were added to the cells at a multiplicity of infection (MOI) of 50, followed by incubation for 3 hours. After incubation, bacteria were removed, and the infected cells were washed three times with plain medium. The cells were further cultured in growth medium under the same conditions. At specific time points, the medium was removed, and the infected cells were washed three times with PBS. DNA was extracted by adding alkaline lysis buffer (25 mM NaOH, 0.2 mM EDTA) directly into the wells, followed by boiling the plates at 95°C for 30 minutes to inactivate the bacteria. The plates were stored at 4°C until further testing.

Bacterial concentration was quantified by qPCR [56]. The primers and TaqMan probe used for the 47 kDa target gene were as follows: 47 kDa FW (5'-TCCAGAATTAAATGAGAATTTAGGAC-3'), 47 kDa RV (5'-TTAGTAATTACATCTCCAG GAGCAA-3'), and 47 kDa probe (5'-FAM-TTCCACATTGTGCTGCAGATCCTTC-TAMRA-3'). The qPCR mixture consisted of 1X qPCR Probe Mix LO-ROX (PCR Biosystems, cat# PB20.21, UK), 0.1 μM of each forward and reverse primer, 0.2

μM probe, sterile distilled water, and 1 μL of extracted DNA. Real-time PCR was performed on a CFX Duet Thermal Cycler (Bio-Rad, USA) using the following conditions: initial denaturation at 95°C for 2 minutes, followed by 45 cycles of 95°C for 15 seconds and 60°C for 30 seconds, with fluorescence acquisition during the annealing/extension phase. DNA copy numbers were calculated by comparison with a standard curve.

In vitro cytokine and chemokine expression analysis

BMDM and human primary macrophages were seeded in 96-well plates at 1×10^4 cells/well and cultured for 24 hours. Cells were either left unstimulated or stimulated for 18 hours with 400 U/ml of recombinant mouse (R&D Systems, cat# 485-MI-100, USA) or human IFN-γ (R&D Systems, cat# 285-IF-100, USA) for BMDM and human primary macrophages, respectively. Bacteria were then added in triplicate after 3 hours, and the infected cells were washed three times with plain medium. Infected cells were further cultured in the presence or absence of IFN-γ for 4 days. The cells were washed three times with PBS and lysed with alkaline lysis buffer. Bacterial concentration was quantified via real-time PCR, as previously described.

Host gene expression was determined by extracting total RNA from BMDM and human primary macrophages using the CellAmp Direct RNA Prep Kit (Takara, cat# 3732, Japan), following the manufacturer's instructions. RNA was transcribed and amplified using the One Step TB Green PrimeScript RT-PCR Kit (Takara, cat# RR066A, Japan). Relative quantitation of mRNA expression was calculated using the 2^(-ΔΔCt) method. Primers are listed in S3 and S4 Tables.

Intracellular infection cycle and ScaC expression analysis

L929 cells were seeded and cultured in μ-Slide 8 Well plates (ibidi, cat# 80826, Germany) at 5×10^3 cells/well for 24 hours. Bacteria were added at an MOI of 50 and incubated for 3 hours. After washing, cells were cultured for 4 and 7 days. On day 4, the number of cells with *Orientia tsutsugamushi* at different subcellular locations was counted, and at day 7, the expression of ScaC was analyzed using immunofluorescence staining. Cells were observed under a confocal microscope, and the data was manually analyzed.

Statistical analysis

All statistical analyses were performed using GraphPad Prism version 10.3.1.

Supporting information

S1 Fig. Additional data from murine infection experiments. A. Kaplan-Meier survival curves of mice infected with $1.25x10^6$ bacteria per animal and monitored for 12 days (low dose experiment). Only strain Kato caused lethality at this dose. Statistical significance was determined using log-rank Mantel-Cox analysis.
(TIF)

S2 Fig. TA686 differs from Karp in its subcellular localisation in HeLa, HUVEC and Rpe1 cell lines. Immunofluorescence microscopy images of TA686 and Karp infected with the same MOI and grown for 4 days. Infected cells were fixed and labelled with an antibody against the abundant surface protein TSA56 (green). Host cell nuclei were labelled with Hoechst (blue). Representative images are shown in A. whilst quantification is given in B. Quantification was performed by manually scoring at least 50 infected cells from three independent replicates. Infected cells were scored as having bacteria in a perinuclear cluster, dispersed throughout the cytoplasm, or in both a perinuclear cluster and dispersed through the cytoplasm.
(TIF)

S1 Table. 16s RNA sequence identity between strains used in this study.
(DOCX)

S2 Table. Tsa56 sequences from NCBI, as determined by megaBLAST on 1 July 2024.
(DOCX)

S3 Table. Nucleotide sequences of oligonucleotide primers for mouse genes.
(DOCX)

S4 Table. Nucleotide sequences of oligonucleotide primers for human genes.
(DOCX)

Acknowledgments

Material has been reviewed by the Walter Reed Army Institute of Research. There is no objection to its publication. The opinions or assertions contained herein are the private views of the author, and are not to be construed as official, or as reflecting true views of the Department of the Army or the Department of Defense. Research was conducted under an IACUC-approved animal use protocol in an AAALAC International - accredited facility with a Public Health Services Animal Welfare Assurance and in compliance with the Animal Welfare Act and other federal statutes and regulations relating to laboratory animals

Author contributions

Conceptualization: Jeanne Salje.

Formal analysis: Manutsanun Inthawong, Erin E. Ball.

Funding acquisition: Jeanne Salje.

Investigation: Panjaporn Chaichana, Naphat Satapoomin, Chitrasak Kullapanich, Suthida Chuenklin, Aisha Mohammad, Piyanate Sunyakumthorn.

Supervision: Jeanne Salje.

Writing – original draft: Jeanne Salje.

Writing – review & editing: Thomas P Burke, Jeanne Salje.

References

1. Luce-Fedrow A, Lehman ML, Kelly DJ, Mullins K, Maina AN, Stewart RL, et al. A Review of Scrub Typhus (Orientia tsutsugamushi and Related Organisms): Then, Now, and Tomorrow. Trop Med Infect Dis. 2018;3(1):8. https://doi.org/10.3390/tropicalmed3010008 PMID: 30274407
2. Watt G, Parola P. Scrub typhus and tropical rickettsioses. Curr Opin Infect Dis. 2003;16(5):429–36. https://doi.org/10.1097/00001432-200310000-00009 PMID: 14501995
3. Xu G, Walker DH, Jupiter D, Melby PC, Arcari CM. A review of the global epidemiology of scrub typhus. PLoS Negl Trop Dis. 2017;11(11):e0006062. https://doi.org/10.1371/journal.pntd.0006062 PMID: 29099844
4. Weitzel T, Dittrich S, López J, Phuklia W, Martinez-Valdebenito C, Velásquez K, et al. Endemic Scrub Typhus in South America. N Engl J Med. 2016;375(10):954–61. https://doi.org/10.1056/NEJMoa1603657 PMID: 27602667
5. Weitzel T, Martínez-Valdebenito C, Acosta-Jamett G, Jiang J, Richards AL, Abarca K. Scrub Typhus in Continental Chile, 2016-20181. Emerg Infect Dis. 2019;25(6):1214–7. https://doi.org/10.3201/eid2506.181860 PMID: 30835200
6. Abarca K, Martínez-Valdebenito C, Angulo J, Jiang J, Farris CM, Richards AL, et al. Molecular Description of a Novel Orientia Species Causing Scrub Typhus in Chile. Emerg Infect Dis. 2020;26(9):2148–56. https://doi.org/10.3201/eid2609.200918 PMID: 32818400
7. Izzard L, Fuller A, Blacksell SD, Paris DH, Richards AL, Aukkanit N, et al. Isolation of a novel Orientia species (O. chuto sp. nov.) from a patient infected in Dubai. J Clin Microbiol. 2010;48(12):4404–9. https://doi.org/10.1128/JCM.01526-10 PMID: 20926708
8. Cho N-H, Kim H-R, Lee J-H, Kim S-Y, Kim J, Cha S, et al. The Orientia tsutsugamushi genome reveals massive proliferation of conjugative type IV secretion system and host-cell interaction genes. Proc Natl Acad Sci U S A. 2007;104(19):7981–6. https://doi.org/10.1073/pnas.0611553104 PMID: 17483455
9. Nakayama K, Yamashita A, Kurokawa K, Morimoto T, Ogawa M, Fukuhara M, et al. The Whole-genome sequencing of the obligate intracellular bacterium Orientia tsutsugamushi revealed massive gene amplification during reductive genome evolution. DNA Res. 2008;15(4):185–99. https://doi.org/10.1093/dnares/dsn011 PMID: 18508905

10. Batty EM, C S, Blacksell SB, Richards A, Paris D, Bowden R, et al. Long-read whole genome sequencing and comparative analysis of six strains of the human pathogen Orientia tsutsugamushi. PLoS Negl Trop Dis. 2018.
11. Giengkam S, Kullapanich C, Wongsantichon J, Adcox HE, Gillespie JJ, Salje J. Orientia tsutsugamushi: comprehensive analysis of the mobilome of a highly fragmented and repetitive genome reveals the capacity for ongoing lateral gene transfer in an obligate intracellular bacterium. mSphere. 2023;8(6):e0026823. https://doi.org/10.1128/msphere.00268-23 PMID: 37850800
12. VieBrock L, Evans SM, Beyer AR, Larson CL, Beare PA, Ge H, et al. Orientia tsutsugamushi ankyrin repeat-containing protein family members are Type 1 secretion system substrates that traffic to the host cell endoplasmic reticulum. Front Cell Infect Microbiol. 2015;4:186. https://doi.org/10.3389/fcimb.2014.00186 PMID: 25692099
13. Beyer AR, VieBrock L, Rodino KG, Miller DP, Tegels BK, Marconi RT, et al. Orientia tsutsugamushi Strain Ikeda Ankyrin Repeat-Containing Proteins Recruit SCF1 Ubiquitin Ligase Machinery via Poxvirus-Like F-Box Motifs. J Bacteriol. 2015;197(19):3097–109. https://doi.org/10.1128/JB.00276-15 PMID: 26170417
14. Beyer AR, Rodino KG, VieBrock L, Green RS, Tegels BK, Oliver LD Jr, et al. Orientia tsutsugamushi Ank9 is a multifunctional effector that utilizes a novel GRIP-like Golgi localization domain for Golgi-to-endoplasmic reticulum trafficking and interacts with host COPB2. Cell Microbiol. 2017;19(7). https://doi.org/10.1111/cmi.12727 PMID: 28103630
15. Evans SM, Rodino KG, Adcox HE, Carlyon JA. Orientia tsutsugamushi uses two Ank effectors to modulate NF-κB p65 nuclear transport and inhibit NF-κB transcriptional activation. PLoS Pathog. 2018;14(5):e1007023. https://doi.org/10.1371/journal.ppat.1007023 PMID: 29734393
16. Adcox HE, Hatke AL, Andersen SE, Gupta S, Otto NB, Weber MM, et al. Orientia tsutsugamushi Nucleomodulin Ank13 Exploits the RaDAR Nuclear Import Pathway To Modulate Host Cell Transcription. mBio. 2021;12(4):e0181621. https://doi.org/10.1128/mBio.01816-21 PMID: 34340535
17. Wangsanut T, Brann KR, Adcox HE, Carlyon JA. Orientia tsutsugamushi modulates cellular levels of NF-κB inhibitor p105. PLoS Negl Trop Dis. 2021;15(4):e0009339. https://doi.org/10.1371/journal.pntd.0009339 PMID: 33857149
18. Atwal S, Wongsantichon J, Giengkam S, Saharat K, Pittayasathornthun YJ, Chuenklin S, et al. The obligate intracellular bacterium Orientia tsutsugamushi differentiates into a developmentally distinct extracellular state. Nat Commun. 2022;13(1):3603. https://doi.org/10.1038/s41467-022-31176-9 PMID: 35739103
19. Chu H, Lee J-H, Han S-H, Kim S-Y, Cho N-H, Kim I-S, et al. Exploitation of the endocytic pathway by Orientia tsutsugamushi in nonprofessional phagocytes. Infect Immun. 2006;74(7):4246–53. https://doi.org/10.1128/IAI.01620-05 PMID: 16790799
20. Kim SW, Ihn KS, Han SH, Seong SY, Kim IS, Choi MS. Microtubule- and dynein-mediated movement of Orientia tsutsugamushi to the microtubule organizing center. Infect Immun. 2001;69(1):494–500. https://doi.org/10.1128/IAI.69.1.494-500.2001 PMID: 11119542
21. Manigrasso G, et al. The intracellular bacterium Orientia tsutsugamushi hijacks the adaptor protein BICD2 for dynein-based motility. Nature Communications (in press). 2024.
22. Rikihisa Y, Ito S. Intracellular localization of Rickettsia tsutsugamushi in polymorphonuclear leukocytes. J Exp Med. 1979;150(3):703–8. https://doi.org/10.1084/jem.150.3.703 PMID: 113480
23. Mika-Gospodorz B, Giengkam S, Westermann AJ, Wongsantichon J, Kion-Crosby W, Chuenklin S, et al. Dual RNA-seq of Orientia tsutsugamushi informs on host-pathogen interactions for this neglected intracellular human pathogen. Nat Commun. 2020;11(1):3363. https://doi.org/10.1038/s41467-020-17094-8 PMID: 32620750
24. Sunyakumthorn P, et al. An intradermal inoculation model of scrub typhus in Swiss CD-1 mice demonstrates more rapid dissemination of virulent strains of Orientia tsutsugamushi. 8(1) thesis, United States, 2013.
25. Hanson B. Comparative susceptibility to mouse interferons of Rickettsia tsutsugamushi strains with different virulence in mice and of Rickettsia rickettsii. Infect Immun. 1991;59(11):4134–41. https://doi.org/10.1128/iai.59.11.4134-4141.1991 PMID: 1718869
26. Thiriot JD, Liang Y, Gonzales C, Sun J, Yu X, Soong L. Differential cellular immune responses against Orientia tsutsugamushi Karp and Gilliam strains following acute infection in mice. PLoS Negl Trop Dis. 2023;17(12):e0011445. https://doi.org/10.1371/journal.pntd.0011445 PMID: 38091346
27. Enatsu T, Urakami H, Tamura A. Phylogenetic analysis of Orientia tsutsugamushi strains based on the sequence homologies of 56-kDa type-specific antigen genes. FEMS Microbiol Lett. 1999;180(2):163–9. https://doi.org/10.1111/j.1574-6968.1999.tb08791.x PMID: 10556707
28. Rights FL, Smadel JE. Studies on scrib typhus; tsutsugamushi disease; heterogenicity of strains of R. tsutsugamushi as demonstrated by cross-vaccination studies. J Exp Med. 1948;87(4):339–51. https://doi.org/10.1084/jem.87.4.339 PMID: 18904219
29. Blacksell SD, Luksameetanasan R, Kalambaheti T, Aukkanit N, Paris DH, McGready R, et al. Genetic typing of the 56-kDa type-specific antigen gene of contemporary Orientia tsutsugamushi isolates causing human scrub typhus at two sites in north-eastern and western Thailand. FEMS Immunol Med Microbiol. 2008;52(3):335–42. https://doi.org/10.1111/j.1574-695X.2007.00375.x PMID: 18312580
30. Tamura A, Takahashi K, Tsuruhara T, Urakami H, Miyamura S, Sekikawa H, et al. Isolation of Rickettsia tsutsugamushi antigenically different from Kato, Karp, and Gilliam strains from patients. Microbiol Immunol. 1984;28(8):873–82. https://doi.org/10.1111/j.1348-0421.1984.tb00743.x PMID: 6438448
31. Robinson DM, Chan TC, Huxsoll DL. Clinical response of silvered leaf monkeys (Presbytis cristatus) to infection with strains of Rickettsia tsutsugamushi virulent and avirulent for mice. J Infect Dis. 1976;134(2):193–7. https://doi.org/10.1093/infdis/134.2.193 PMID: 823272
32. Wang G, Fu R, Zhang L, Xue L, Al-Mahdi AY, Xie X, et al. Genomic bacterial load associated with bacterial genotypes and clinical characteristics in patients with scrub typhus in Hainan Island, Southern China. PLoS Negl Trop Dis. 2023;17(4):e0011243. https://doi.org/10.1371/journal.pntd.0011243 PMID: 37083859

33. Kim D-M, Yun NR, Neupane GP, Shin SH, Ryu SY, Yoon HJ, et al. Differences in clinical features according to Boryoung and Karp genotypes of Orientia tsutsugamushi. PLoS One. 2011;6(8):e22731. https://doi.org/10.1371/journal.pone.0022731 PMID: 21857951
34. Ge Y, Rikihisa Y. Subversion of host cell signaling by Orientia tsutsugamushi. Microbes Infect. 2011;13(7):638–48. https://doi.org/10.1016/j.micinf.2011.03.003 PMID: 21458586
35. Trent B, Fisher J, Soong L. Scrub Typhus Pathogenesis: Innate Immune Response and Lung Injury During Orientia tsutsugamushi Infection. Front Microbiol. 2019;10:2065. https://doi.org/10.3389/fmicb.2019.02065 PMID: 31555249
36. Münch CC-S, Upadhaya BP, Rayamajhee B, Adhikari A, Münch M, En-Nosse N, et al. Multiple Orientia clusters and Th1-skewed chemokine profile: a cross-sectional study in patients with scrub typhus from Nepal. Int J Infect Dis. 2023;128:78–87. https://doi.org/10.1016/j.ijid.2022.12.022 PMID: 36566774
37. Astrup E, Janardhanan J, Otterdal K, Ueland T, Prakash JAJ, Lekva T, et al. Cytokine network in scrub typhus: high levels of interleukin-8 are associated with disease severity and mortality. PLoS Negl Trop Dis. 2014;8(2):e2648. https://doi.org/10.1371/journal.pntd.0002648 PMID: 24516677
38. Kang S-J, Jin H-M, Cho Y-N, Kim SE, Kim UJ, Park K-H, et al. Increased level and interferon-γ production of circulating natural killer cells in patients with scrub typhus. PLoS Negl Trop Dis. 2017;11(7):e0005815. https://doi.org/10.1371/journal.pntd.0005815 PMID: 28750012
39. Iwasaki H, Takada N, Nakamura T, Ueda T. Increased levels of macrophage colony-stimulating factor, gamma interferon, and tumor necrosis factor alpha in sera of patients with Orientia tsutsugamushi infection. J Clin Microbiol. 1997;35(12):3320–2. https://doi.org/10.1128/jcm.35.12.3320-3322.1997 PMID: 9399546
40. Chierakul W, de Fost M, Suputtamongkol Y, Limpaiboon R, Dondorp A, White NJ, et al. Differential expression of interferon-gamma and interferon-gamma-inducing cytokines in Thai patients with scrub typhus or leptospirosis. Clin Immunol. 2004;113(2):140–4. https://doi.org/10.1016/j.clim.2004.08.006 PMID: 15451469
41. Kristof MN, Allen PE, Yutzy LD, Thibodaux B, Paddock CD, Martinez JJ. Significant Growth by Rickettsia Species within Human Macrophage-Like Cells Is a Phenotype Correlated with the Ability to Cause Disease in Mammals. Pathogens. 2021;10(2):228. https://doi.org/10.3390/pathogens10020228 PMID: 33669499
42. Curto P, Simões I, Riley SP, Martinez JJ. Differences in Intracellular Fate of Two Spotted Fever Group Rickettsia in Macrophage-Like Cells. Front Cell Infect Microbiol. 2016;6:80. https://doi.org/10.3389/fcimb.2016.00080 PMID: 27525249
43. Liang Y, Wang H, Sun K, Sun J, Soong L. Lack of the IFN-γ signal leads to lethal Orientia tsutsugamushi infection in mice with skin eschar lesions. PLoS Pathog. 2024;20(5):e1012020. https://doi.org/10.1371/journal.ppat.1012020 PMID: 38743761
44. Burke TP, Engström P, Chavez RA, Fonbuena JA, Vance RE, Welch MD. Inflammasome-mediated antagonism of type I interferon enhances Rickettsia pathogenesis. Nat Microbiol. 2020;5(5):688–96. https://doi.org/10.1038/s41564-020-0673-5 PMID: 32123346
45. Burke TP, Engström P, Tran CJ, Langohr IM, Glasner DR, Espinosa DA, et al. Interferon receptor-deficient mice are susceptible to eschar-associated rickettsiosis. Elife. 2021;10:e67029. https://doi.org/10.7554/eLife.67029 PMID: 34423779
46. Hotta K, Pham HTT, Hoang HT, Trang TC, Vu TN, Ung TTH, et al. Prevalence and Phylogenetic Analysis of Orientia tsutsugamushi in Small Mammals in Hanoi, Vietnam. Vector Borne Zoonotic Dis. 2016;16(2):96–102. https://doi.org/10.1089/vbz.2015.1831 PMID: 26771283
47. Cosson JF, Galan M, Bard E, Razzauti M, Bernard M, Morand S, et al. Detection of Orientia sp. DNA in rodents from Asia, West Africa and Europe. Parasit Vectors. 2015;8:172. https://doi.org/10.1186/s13071-015-0784-7 PMID: 25884521
48. Tamura A, Yamamoto N, Koyama S, Makisaka Y, Takahashi M, Urabe K, et al. Epidemiological survey of Orientia tsutsugamushi distribution in field rodents in Saitama Prefecture, Japan, and discovery of a new type. Microbiol Immunol. 2001;45(6):439–46. https://doi.org/10.1111/j.1348-0421.2001.tb02643.x PMID: 11497219
49. Walker JS, Chan CT, Manikumaran C, Elisberg BL. Attempts to infect and demonstrate transovarial transmission of R. tsutsugamushi in three species of Leptotrombidium mites. Ann N Y Acad Sci. 1975;266:80–90. https://doi.org/10.1111/j.1749-6632.1975.tb35090.x PMID: 829478
50. Schön ME, Martijn J, Vosseberg J, Köstlbacher S, Ettema TJG. The evolutionary origin of host association in the Rickettsiales. Nat Microbiol. 2022;7(8):1189–99. https://doi.org/10.1038/s41564-022-01169-x PMID: 35798888
51. Verhoeve VI, Lehman SS, Driscoll TP, Beckmann JF, Gillespie JJ. Metagenome diversity illuminates origins of pathogen effectors. bioRxiv. 2023. https://doi.org/10.1101/2023.02.26.530123 PMID: 36909625
52. Elliott I, Thangnimitchok N, de Cesare M, Linsuwanon P, Paris DH, Day NPJ, et al. Targeted capture and sequencing of Orientia tsutsugamushi genomes from chiggers and humans. Infect Genet Evol. 2021;91:104818. https://doi.org/10.1016/j.meegid.2021.104818 PMID: 33771726
53. Chen K, Travanty NV, Garshong R, Crossley D, Wasserberg G, Apperson CS, et al. Detection of Orientia spp. Bacteria in Field-Collected Free-Living Eutrombicula Chigger Mites, United States. Emerg Infect Dis. 2023;29(8):1676–9. https://doi.org/10.3201/eid2908.230528 PMID: 37486323
54. Giengkam G, et al. Orientia tsutsugamushi: analysis of the mobilome of a highly fragmented and repetitive genome reveals ongoing lateral gene transfer in an obligate intracellular bacterium. mSphere. 2023.
55. Giengkam S, Blakes A, Utsahajit P, Chaemchuen S, Atwal S, Blacksell SD, et al. Improved Quantification, Propagation, Purification and Storage of the Obligate Intracellular Human Pathogen Orientia tsutsugamushi. PLoS Negl Trop Dis. 2015;9(8):e0004009. https://doi.org/10.1371/journal.pntd.0004009 PMID: 26317517
56. Salje J. Quantifying Orientia tsutsugamushi and other Rickettsiales bacteria by real time qPCR. 2025. *protocols.io*, https://doi.org/10.17504/protocols.io.8epv5nz4jv1b/v1